## Ferroelectrics

# Structural Phase Transitions and Solid State Chemical Reactions in Complex Potassium Hydrogen Sulfate Salts Driven by Fast Proton Diffusion

A. I. Baranov [a] , V. V. Grebenev [a] , U. BismaYer [b] & J. Ludwig [b]

[a] Institute of Crystallography, Russian Academy of Sciences , 117333, Leninskii pr. 59, Moscow, Russia

[b] Mineralogisch-Petrographisches Institut, Universität Hamburg , 20146, Hamburg, Grindelallee 48, Germany
Published online: 20 Sep 2010.

PLEASE SCROLL DOWN FOR ARTICLE

Taylor & Francis
Taylor & Francis Group

# Structural Phase Transitions and Solid State Chemical Reactions in Complex Potassium Hydrogen Sulfate Salts Driven by Fast Proton Diffusion

A. I. BARANOV,[1,*] V. V. GREBENEV,[1,**] U. BISMAYER,[2]
AND J. LUDWIG[2]

[1]Institute of Crystallography, Russian Academy of Sciences, 117333, Leninskii
pr. 59, Moscow, Russia
[2]Mineralogisch-Petrographisches Institut, Universität Hamburg, 20146
Hamburg, Grindelallee 48, Germany

*At elevated temperatures the crystals of complex acid salts $K_mH_n(SO_4)_{(m+n)/2}xH_2O$*
*($0 \leq x \leq 1, m > 3, n \geq 1$) exhibit an anomalous temperature behavior of the dielectric*
*permittivity and conductivity similar to the behavior observed in pure $KHSO_4$ at the*
*structural phase transition or on melting. This unusual behavior is due to the formation*
*of multiphase states at higher temperatures where phases with different chemical com-*
*position coexist. It is shown that $K_3H(SO_4)_2$ undergoes a ferroelastic phase transition*
*between the point groups $3\bar{m} \leftrightarrow 2/m$ with anomalously slow kinetics at 463 K while the*
*multiphase state is formed near 480 K*

**Keywords**   Phase transitions; ferroelastics; proton dynamics; domain structure

## 1. Introduction

Most hydrogen bonded crystals with general formula $Me_nH_m(XO_4)_{(m+n)/2}$ (M = K, Cs, Rb, $NH_4$ and X = S, Se) are interesting because of their variety of phase transitions which are due to the complex disorder of the proton subsystem. Most of those crystals undergo low temperature ferroelectric or antiferroelectric phase transitions with an ordering of the protons in double well potentials. At high temperatures they show ferroelastic phase transitions, which are accompanied by the delocalization of protons and dynamical disordering of the H-bond network. Moreover, the fast proton diffusion and the disordered hydrogen bond network are responsible for some peculiarities of the structural transformation in these compounds.

It is well known that crystals of $K_3H(SeO_4)_2$ $Rb_3H(SeO_4)_2$ and $(NH_4)_3H(SeO_4)_2$ with space group A2/a are ferroelastic at room temperature and undergo a phase transition to a prototype phase with space group $R\bar{3}m$ [1–3]. Simultaneously this phase transition is superprotonic because it is accompanied by large changes (about four orders of magnitude)

of the protonic conductivity. It was however shown recently, that structurally isomorphous $K_3H(SO_4)_2$ shows quite different ferroelastic properties at elevated temperatures [4, 5]. In particularly, X-ray diffraction experiments show that the structure of $K_3H(SO_4)_2$ in the high temperature phase cannot be identified as trigonal or hexagonal [5]. An endothermic DSC signal was observed at the phase transition temperature $T = 479$ K with corresponding enthalpy $\Delta H = 18.4$ kJ/mol and entropy $\Delta S = 4.6R$ [4]. Those values are considerably larger than the corresponding values of these parameters at ferroelastic phase transitions in other structurally isomorphous crystals. For example, at the ferroelastic phase transitions in $Rb_3H(SeO_4)_2$ $\Delta H = 4.4$ kJ/mol and $\Delta S = 1.1R$ [6]. On the other hand the transition temperature in $K_3H(SO_4)_2$ coincides with the melting temperature of simple $KHSO_4$. Moreover, the values $\Delta S = 4.4R$ and $\Delta H = 17.6$ kJ/mol at the melting point of $KHSO_4$ are close to those at the phase transition of $K_3H(SO_4)_2$ [7].

A detailed study of the peculiarities of the ferroelastic properties and structural phase transitions of $K_3H(SO_4)_2$ is the subject of this work. In addition, the crystals $K_9H_7(SO_4)_8 \cdot H_2O$ and $KHSO_4$ were also studied for complementary information.

## 2. Experimental

$K_3H(SO_4)_2$ (TKHS) and $K_9H_7(SO_4)_8 \cdot H_2O$ (NKHS) and $KHSO_4$ (KHS) single crystals were grown from saturated water solutions by slow evaporation. Measurements of the complex admittance were carried out at the frequency of 1 MHz in the temperature range of 290–500 K. Two different temperature treatments were used: 1) a continuous change of the temperature with heating and cooling rate about 20 K/hour; 2) a temperature stabilization regime where the required thermal stabilization was determined by reaching equilibrium values of the admittance. Plate-like samples were cut perpendicular to the different crystallographic directions. Silver paste was used as electrodes.

The optical polarization technique was used for a visual study of TKHS single crystalline plates in the temperature range of 290–500 K at the different temperature regimes.

The X-ray powder diffraction experiments were carried out in the temperature range 290–520 K using a Philips X-pert diffractometer ($CuK_{\alpha 1}$ radiation, Si (111)).

## 3. Experimental Results

### 3.1. Conductivity Study

Temperature dependences of the ac conductivity for single crystalline TKHS samples were measured for different heating regimes shown in Fig. 1. An abruptly increasing conductivity of more than three orders of magnitude is observed at $T_I^+ = 480$ K (Fig. 1, curve1) on continuous heating. It should be noted that a similar strong increase of the conductivity is typical for superionic phase transitions. During first heating in the temperature stabilization regime an additional large anomaly of the conductivity occurs at $T_{II}^+ = 463$ K (curve 2). This jump of the conductivity was obtained during a stabilization time of about 9 hours at 463 K. However, on repeated heating the anomaly of the conductivity at $T_{II}^+$ arises even on continuous heating (20 K/h). Moreover, both anomalies of the conductivity at $T_I^+ = 480$ K and $T_{II}^+ = 463$ K also occur in polycrystalline pellets upon continuous heating. Significantly smaller anomalies were observed at $T_I^- = 440$ K and $T_{II}^- = 420$ K also upon cooling. The jumps of the conductivity at these temperatures are much smaller than on heating (Fig. 1 curves 1, 2).
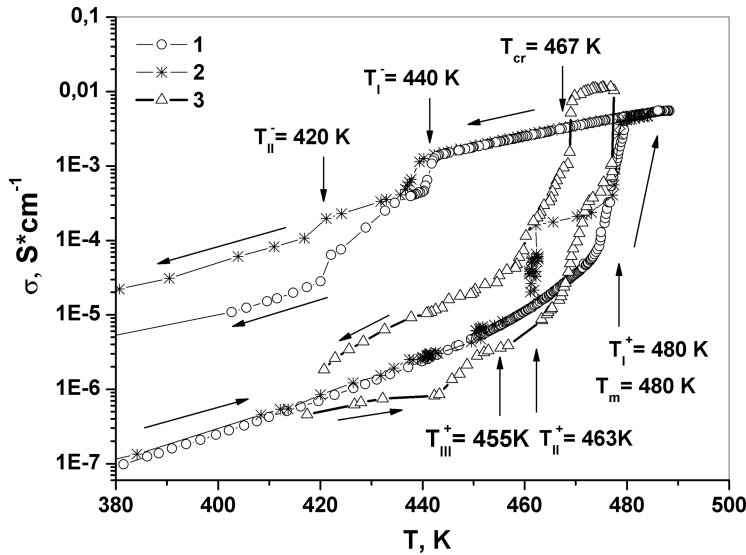
**Figure 1.** Temperature dependences of the conductivity upon heating and cooling single crystal samples of $K_3H(SO_4)_2$ [100] (curves 1,2) and $KHSO_4$ [100] (curve 3) measured at a frequency of 1 MHz. 1,3-continuous heating; 2-heating in the thermal stabilization regime. Symbols $T_m$ and $T_{cr}$ correspond only to $KHSO_4$.

Figure 1 also shows the temperature dependences of the conductivity for [100] direction of $KHSO_4$ (curve 3). It can be seen that $KHSO_4$ shows a strong anomaly of the conductivity at $T_I^+= 480$ K. Moreover, this anomaly is quantitatively similar to the one observed for single crystals of TKHS at the same temperature $T_I^+$(curves 1 and 3). It should be noted that according to visual observation (because of changes of the geometrical form of the sample) the temperature $T_I^+$ corresponds to the melting temperature $T_m$ of KHS [7]. On cooling crystallization of KHS occurs at $T_{cr} = 467$ K. Furthermore $KHSO_4$ shows another well-defined anomaly of the conductivity at $T_{tr} = T_{III}^+ = 455 \pm 5$ K, which corresponds to its reversible structural phase transition [7, 10].

It is interesting that the complex salt NKHS also shows an anomalous increase of the conductivity at temperatures $T_{sp}$, $T_I^+$ and $T_{II}^+$ (Fig. 2). It was shown earlier [8] that the anomaly at the temperature $T_{sp}$ corresponds to the superprotonic phase transition which is accompanied by a loss of structural water. The reversibility of this phase transition and restoring of the initial chemical composition of NKHS are controlled by the absorption kinetics of atmospheric water at temperatures $T < T_{sp}$. The shape of the conductivity curve at $T_{II}$ and peculiarities of it temperature hysteresis suggests that this anomaly corresponds to the one observed at the reversible structural transition $T_{tr}$ in KHS. Fig. 2 shows that at $T_I^+$ and $T_I^-$ NKHS reveals anomalies of the conductivity similar to those observed for TKHS at the same temperatures and for KHS on melting.

Summarizing the result above we can conclude that the crystals KHS, TKHS and NKHS show similar anomalous behavior of the conductivity at characteristic temperatures: $T_I^+$ and $T_{II}^+$. Moreover, these temperatures correspond to the melting temperature $T_m$ and the structural phase transition point $T_{tr}$ in KHS.
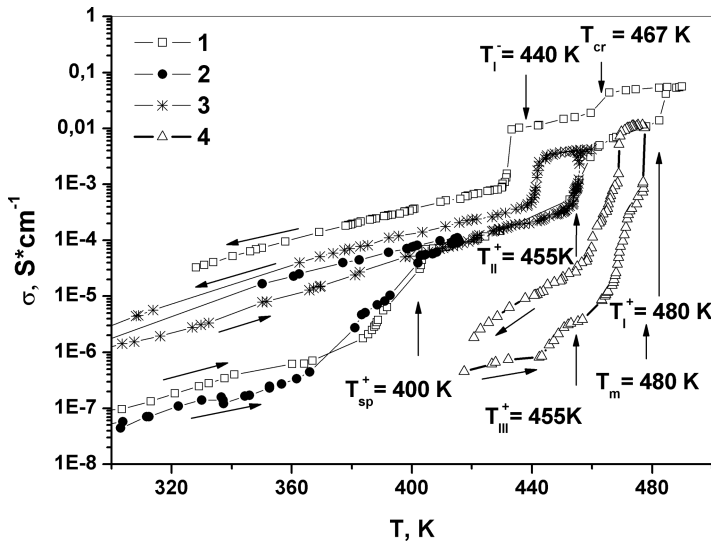
**Figure 2.** Temperature dependences of the conductivity upon heating and cooling single crystal samples of $K_9H_7(SO_4)_8 \cdot H_2O$ [100] (curves 1 – 3) and $KHSO_4$ [100] (curve 4) measured on continuous heating at frequency 1MHz. 1- heating –cooling cycle in the temperature range 290-590 K; 2- heating –cooling cycle in the temperature range 290-420 K; 3- heating –cooling cycle in the temperature range 290–460 K; 4- heating –cooling cycle in the temperature range 410–480 K. Symbols $T_m$ and $T_{cr}$ correspond only to $KHSO_4$.

### 3.2. Optical Study

Polarizing microscope observations confirm the existence of an as-grown ferroelastic domain structure in TKHS [3, 4]. The analysis of extinction positions and orientations of the domain walls in (001) and (010) plates indicate the existence of three orientation states in the monoclinic phase and suggest the point group symmetry of the prototype phase to be $\bar{3}m$. Our conclusion agrees with previous results of Chen et al. [3]. Upon continuous heating using the rate dT/dt >10 K/hour the domain structure disappears at the temperature $T_I^+$. However, the scheme of the disappearing domain structure in TKHS is quite different from that observed in classical ferroelastic phase transitions. On the first sight the disappearance of the domains is due to an abruptly occurring thermal decomposition which leads to turbidity of the sample. However, on slower heating a regular needle structure appears at T $\geq T_{III}$ and disappears at T $\approx T_I$ (Fig. 3). The needles are oriented along defined crystallographic directions and can be observed in both (001) and (010) planes. Most probably these needles correspond to a new phase. Upon cooling from temperatures $T > T_I$ the domain structure appears as well as the needles disappear. After cooling the sample retains opaque at room temperature. Only after polishing the sample the texture with irregular boundaries reappears. The extinction positions of these areas correspond to 60° symmetry. Besides, regions with needle structure also become visible in polarized light. Thus, after heating above $T_I \geq 480$ K surface layer of the sample becomes polycrystalline and opaque but the bulk of the sample retains clear and crystalline.

In the thermal stabilization regime TKHS shows a quite different temperature behavior. Fig. 4 (image 1) shows the as-grown sample with two orientation states at room temperature. When the temperature is stabilized at $T = T_{II}$ the phase front appears on the edge of the
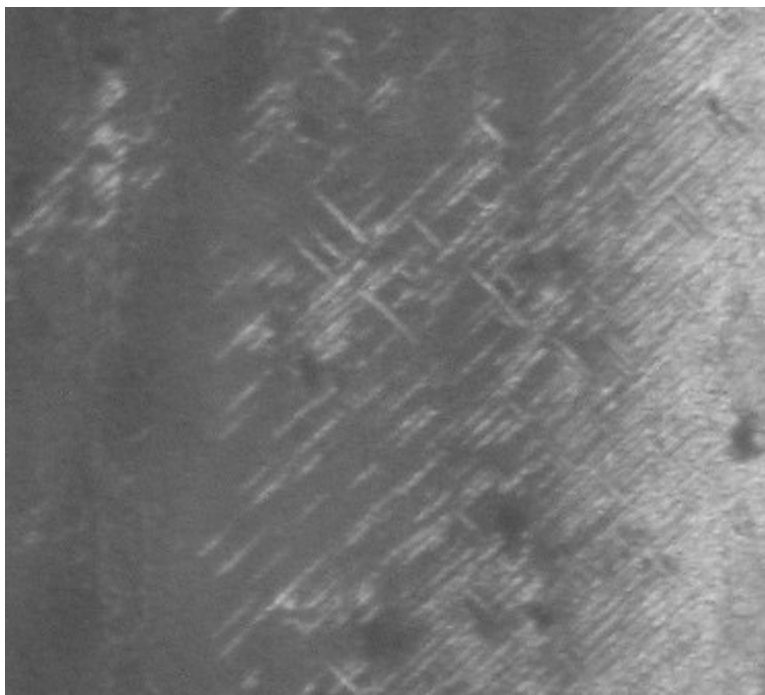
**Figure 3.** Crossed polarizer microscope images of (001) plates of the as-grown sample $K_3H(SO_4)_2$ at different temperatures obtained on continuous heating. 1- needle inclusions at T = 470 K. 2. T = $T_I$ = 480 K.

sample. This front has arbitrary orientation relative to the crystallographic directions, it moves from the edges of the sample and separates the initial monoclinic optically biaxial phase and a new optically uniaxial phase (Fig. 4, image 2). The very slow moving phase boundary suggests that the phase transition is driven by diffusion. Taking into account the structural peculiarities of TKHS we may conclude that only protons contribute to this
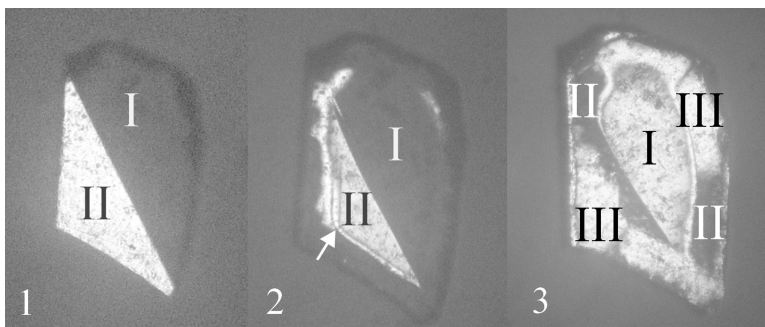


**Figure 4.** Crossed polarizer microscope images of (001) plate of the as-grown sample $K_3H(SO_4)_2$ at T = 470 K obtained on continuous heating. 1-domain structure of the as-grown sample at room temperature T = 290 K. 2- T = $T_{II}^+$ = 463 K, the phase front between the new optically uniaxial and as-grown monoclinic phase is shown by arrow. 3- Domain structure after cooling from T = 467 K. Roman symbols denote orientational states.

www.m

diffusion process. Using results of the optical observations the diffusion coefficient can be estimated as

$$D = \triangle l^2 / \triangle t, \tag{1}$$

where $\Delta l$ is the displacement of the phase boundary in the time interval $\Delta t$. The obtained value D $\approx 3 \cdot 10^{-7}$ cm$^2$/sec is close to the value calculated from the experimental value of the conductivity TKHS at $T_{II}^+$ according to

$$D = \frac{\sigma kT}{nq^2} \approx 1 \cdot 10^{-7} \text{cm}^2/\text{sec} \tag{2}$$

where $n$ is the concentration of mobile protons with $n = 6.4 \cdot 10^{21}$cm$^{-3}$, $q$ is the proton charge and $k$ is the Boltzmann constant.

The phase transition at $T_{II}$ was not completed in our experiments. Therefore, in the temperature range $T_{II}^+ - T_I^+$ the initial monoclinic phase and the new phase coexist (Fig. 4, image 2). Upon cooling in the crystal area of the optically uniaxial phase a new domain structure arises below $T_{II}^-$ (Fig. 4, image 3). Unlike the as-grown domain structure the new domain structure shows arbitrary oriented and fuzzed domain boundaries. However, the extinction positions of the new domains coincide with the extinction positions of the domains of the as-grown sample. Thus, the results of the optical study indicate trigonal symmetry of the new phase which transforms in a monoclinic phase at temperature $T_{II}^-$ and retransforms back at $T_{II}^+$. This reversible ferroelastic phase transition is typical for an anomalously slow kinetics.

Our optical study of NKHS did not yield useful information on domain patterns, because above the temperature of the superprotonic phase transition $T_{sp}$ the crystal becomes milky white and hence, the phase transformation at $T_{II}$ is not visible. Upon heating to $T_I$ traces of melting appear.

### 3.3. X-Ray Diffraction Study

X-ray diffraction data for TKHS were collected at temperatures, which are close to the thermal stabilization regime in the conductivity and optical experiments. Figure 5 shows that X-ray powder diffraction patterns of TKHS begin to change at T = 443 K (slightly below $T_{II}^+$) and completely change at $T_{II}^+$ and $T_I^+$. Above $T_{II}^+$ powder patterns of TKHS indicate a multiphase state and hence, they are difficult to analyse. Nevertheless, some peaks of $K_2SO_4$ can be identified in the temperature interval $T_{II}^+ < T < T_I^+$. Residual peaks can be attributed to the trigonal phase of TKHS and the high temperature phase of KHS. The presences of peaks of $K_2SO_4$ suggest that the ferroelastic phase transition at $T_{II}$ is accompanied by a solid-state reaction. Unfortunately a precise diffraction pattern solution is impossible because no structural data of the high temperature phase KHS are available [9]. The X-ray patterns indicate however complete reversibility of the ferroelastic phase transition upon cooling in the temperature interval $T_{II}^+ < T < T_I^+$.

X-ray diffraction data at $T > T_I^+$ show that most Bragg-peaks of the unknown phase disappear and are replaced by peaks of the $K_2S_2O_7$ phase. Moreover, the high temperature phase of TKHS ($T > T_I$) appears to be a mixture of $K_2SO_4$ and $K_2S_2O_7$. However, at these temperatures the powder diffraction pattern cannot completely be described by a simple two-phase mixture model. This may be due to low accuracy structure data of $K_2S_2O_7$ [10]. The structural transformation at $T_I^+$ is not completely reversible and the powder diffraction
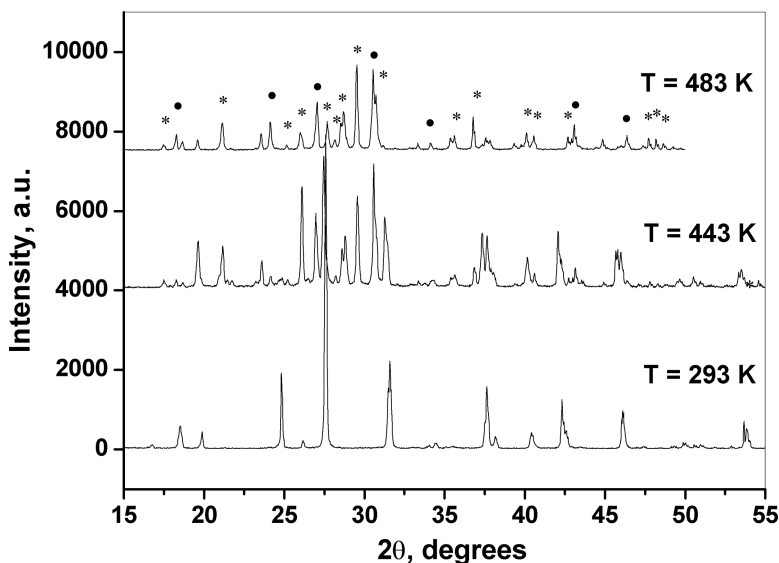
*A.I. Baranov et al.*

**Figure 5.** X-ray powder diffraction patterns: 1. $K_3H(SO_4)_2$ at room temperature, $T = 293$ K. 2. $K_3H(SO_4)_2$, $T = 443$ K. 3. $K_3H(SO_4)_2$, $T = 483$ K ($K_2S_2O_7$ phase indicated by dots and $K_2SO_4$ phase marked by stars)

pattern of the sample only slightly changes upon cooling below $T_I^-$. Thus, above $T_I^+$ thermal decomposition of TKHS takes place accompanied by an irreversible lost of water.

## 4. Discussion

The obtained results indicate that TKHS undergoes a reversible ferroelastic phase transition at $T_{II}^+ = 463$ K with a change of the point group symmetry $\bar{3}m \leftrightarrow 2/m$. The distinctive feature of this phase transition which deviates from other crystals of the $Me_nH_m(XO_4)_{(m+n)/2}$ family is its anomalously slow kinetics. Because of this peculiarity the ferroelastic monoclinic phase and the prototype trigonal phase coexists at $T > T_{II}$. The broad phase boundary, its arbitrary orientation and the estimated value of the diffusion coefficient $D \approx 10^{-7}$ cm$^2$/sec suggest that the phase transition involves proton diffusion. From the structure of TKHS and its transformation with symmetry change $\bar{3}m \leftrightarrow 2/m$ the velocity of the phase boundary might be expected to be close to the velocity of sound. Therefore, it is most probable that a solid-state chemical reaction accompanies the ferroelastic phase transition in TKHS and limits the rate of the structural transformation. On the other hand, the rate of such a reaction will be determined by the diffusion of protons. The decreasing intensity of the diffraction peaks of TKHS and the increase of those of $K_2SO_4$ confirms this suggestion. Unfortunately, because of the lack of structural data of the high temperature phase of $KHSO_4$ the high temperature pattern could not be identified unambiguously and hence, we cannot proof the existence of $KHSO_4$ at higher temperatures. The high temperature compound is expected to be a product of the solid-state chemical reaction, driven by fast proton diffusion:

$$K_3H(SO_4)_2 = (KHSO_4 \cdot K_2SO_4) \rightarrow K_2SO_4 + KHSO_4 \qquad (3)$$
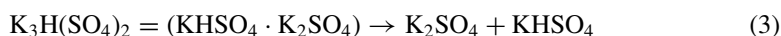
In this case melting of the KHS phase imbedded into a TKHS-matrix may cause the sharp increase of the conductivity at $T_I^+$.

<div align="center">

**Table 1**

</div>

Temperatures (in K) of the phase transitions of complex salts. Phase transitions and melting temperatures of simple salts for some crystals of the $Me_mH_n(SO_4)_{(m+n)/2}$ family.

| Compound | $T_{tr}$ in $Me_mH_n(SO_4)_{(m+n)/2}$ | $T_m/T_{tr}$ of $MeHAO_4/Me_2SO_4$ |
|---|---|---|
| $K_3H(SO_4)_2$ | 480 ($\pm$1) $T_I$ | $KHSO_4$ 480 ($\pm$2) $T_m$ [7] |
| $K_9H_7(SO_4)_8 \cdot H_2O$ | 455 ($\pm$1) $T_{II}$ | $KHSO_4$ 455 ($\pm$2) $T_{III}$ [9] |
| $K_9H_7(SO_4)_8 \cdot H_2O$ | 480 ($\pm$1) $T_I$ | $KHSO_4$ 480 ($\pm$2) $T_m$ [7] |
| $Cs_5H_3(SO_4)_4 \cdot xH_2O$ | 414 ($\pm$1) $T_{sp}$ [11] | $CsHSO_4$ 414 ($\pm$1) $T_{sp}$ [12] |
| $Cs_3H(SO_4)_2$ | 419 ($\pm$2) $T_{sp}$ [13] | $CsHSO_4$ 414 ($\pm$1) $T_{sp}$ [12] |
| $Na_3H(SO_4)_2$ | 505 ($\pm$1) $T_{sp}$ [14] | $Na_2SO_4$ 507 ($\pm$1) III-II [15] |

Further confirmation of the formation of the KHS phase is the coincidence of the melting temperature of KHS $T_m$ and the temperature of the anomalous increase of the conductivity TKHS $T_I^+$ (Fig. 1). Decomposition of the complex salt into simple salts is also confirmed by the conductivity data of NKHS (Fig. 2). For this crystal the coincidence of the temperatures of the conductivity anomalies at $T_{II}^+$ and $T_I^+$ with the temperatures of the structural phase transition $T_{tr}$ and melting $T_m$ of KHS is not occasional. Moreover, literature data indicate that there are other complex salts that reveal physical properties of the simple salts such as the superprotonic phase transition and melting (Table 1). The decomposition process of the complex salt is possible because the complex as well as the simple salts consist of similar structural units and differ only by the network of hydrogen bonds. Therefore, dynamically disordering of the hydrogen bond network of the complex salt is favored to form structural configurations which correspond to arrangements in the simple salts.

## 5. Conclusion

It was shown that the ferroelastic phase transition in TKHS occurs at $T = 463$ K rather than at $T = 480$ K as had been described earlier [4, 5]. Unlike the isostructural ferroelastic phase transitions $2/m \leftrightarrow \bar{3}m$ observed in most crystals of $Me_3H(XO_4)_2$, the phase transition in TKHS is characterized by an anomalously slow kinetics that makes its experimental detection difficult. The obtained results suggest that the kinetics of the latter phase transition is determined by interplay of two phenomena: fast proton diffusion and solid state chemical reaction. Such solid-state chemical reactions also accompany structural transformations in other complex salts of the hydrogen sulphate family.

## References

1. K. Aizu, *Rev.* B2 754–758 (1970.)
2. R. H. Chen, R. Y. Chang, C. S. Shern, *J. Phys. Chem. Solids.* **63**, 2069–2075 (2002).
3. R. H. Chen and T. M. Chen, *J. Phys. Chem. Solids.* **58**, 161–170 (1997).
4. R. H. Chen, R. Y. Chang, C. S. Shern, and T. J. Fukami, *Phys. Chem. Solids* **64**, 53–563 (2003).
5. R. I. Chisholm Calum and S. M. Haile *Solid State Ionics.* **145**, 179–184 (2001).
6. A. I. Baranov, I. P. Makarova, L. A. Muradyan, A. V. Tregubchenko, L. A. Shuvalo, and V. I. Simonov, *Sov. Phys. Crystallogr.* **32**(3) 400–406 ( 1987).
7. E. Rapoport, et al., *High Temp. High Pressure.* **30**, 183–187 (1979).

8. A. I. Baranov, V. V. Sinitsyn, V. Yu. Vinnichenko, D. J. Jones, and B. Bonnet, *Sol. St. Ionics.* **97** 153–160 (1998)

9. G. Y. Lentz, K. Knorr, W. Depmeier, C. Baehtz, M. Knapp, and W. Morgenroth, *Desy annual reports.* **41**(1), 8150–8151 (2002).

10. K. Ståhl, T. Balic-Zunic, F. da Silva, K. M. Eriksen, R. W. Berg, and R. Fehrmann, *Solid State Chemistry.* **178** (5), 1697–1704 ( 2005).

11. A. I. Baranov, B. V. Merinov, V. S. Ryabkin, and E. P. Efremova, *Ferroelectrics*, **302** 29–35 (2004).

12. A. I. Baranov, L. A. Shuvalov,and N. M. Shchagina, *Pis'ma Zh. Éksp. Teor. Fiz.* **36**, 381–387 [*JETP Lett.* **36**, 459–467 (1982)] (1982).

13. A. R. Lim, *Phys Rev.* B72 064103-1-064103-6 (2005).

14. R. H. Chen, R.-J. Wang, T. Fukami, C. S. Shern, *Solis State Ionics* **110**(3–4), 277–281 ( 1998).

15. B.-K. Choi and D. J. Lockwood, *J. Phys. Condens. Matter.* **17**, 6095–6108 (2005).